

A comparison of experimental buckling load of rectangular plates determined from various measurement methods

ชวรินทร์ สุภาศักดิ์ ไพโรจน์ สิงหนัดกิจ
ภาควิชาวิศวกรรมเครื่องกล คณะวิศวกรรมศาสตร์ จุฬาลงกรณ์มหาวิทยาลัย
เขตปทุมวัน กรุงเทพฯ 10330
โทร: 0-2218-6595 โทรสาร: 0-2252-2889 E-mail: Pairod.S@chula.ac.th

Chavanan Supasak, Pairod Singhatanadgid
Department of Mechanical Engineering, Faculty of Engineering, Chulalongkorn University,
Bangkok, 10330, Thailand
Tel: 0-2218-6595 Fax: 0-2252-2889 E-mail: Pairod.S@chula.ac.th

Abstract

In this study, rectangular aluminum plates are loaded on an in-house designed unidirectional compression-testing machine. Buckling load of aluminum rectangular plates are determined using four different techniques, i.e. (1) a plot of applied load vs. out-of-plane displacement, (2) a plot of applied load vs. end shortening, (3) a plot of applied load vs. average in-plane strain, and (4) the Southwell plot. The experimental results suggest that a plot of average strain gives the most reliable buckling load, compared to the theoretical solutions. The plots of out-of-plane displacement and end shortening produce a good tendency of buckling load from specimen to specimen. On the other hand, the Southwell plot is the less dependable technique. It is observed that technique 1, 2, and 4 are affected by the imperfection of the test setup. More tests are required so that more reliable conclusions can be reached.

1. Introduction

In many engineering structures such as columns, beams, or plates, their failure develops not only from excessive stresses but also from buckling. Only rectangular thin plates are considered in the present study. When a flat plate is subjected to low in-plane compressive loads, it remains flat and is in equilibrium condition. As the magnitude of the in-plane compressive load increases, however, the equilibrium configuration of the plate is eventually changed to a non-flat configuration and the plate becomes unstable. The magnitude of the compressive load at which the plate becomes unstable is called the "critical buckling load." For simply supported rectangular isotropic plates, buckling load can be solved analytically, and written as a closed-form solution [1].

Besides analytical study, there are several experimental studies on buckling of rectangular plates. Chai *et al.* [2] investigated the laminated plates under unidirectional loading using LVDT and strain gage to measure the out-of-plane deflection and in-plane strain, respectively. The buckling loads from experiment well correlate with finite element solutions. Discrepancies between -7% and 11% of the experimental buckling loads were reported. Also, Laser-based holography and strain gauges were used to measure buckling behavior and compared with the numerical results by Chai *et al.* [3]. Tuttle *et al.* [4] determined buckling loads from plots of applied load vs. out-of-plane displacement. Shadow moiré technique method was used to monitor the whole-field out-of-plane deflections of the buckled plates. The maximum out-of-plane displacement was measured by placing a dial indicator on the specimen.

There are several techniques used in buckling experiments of flat plates. It is necessary to know the advantages and disadvantages of each method. Therefore, in the present study, buckling loads determined from four different experiment methods were compared with the theoretical buckling loads. The four methods [5] studied in this paper are a) plot of applied load vs. out-of-plane displacement b) plot of applied load vs. end shortening c) plot of applied load vs. average in-plane strain, and, d) the Southwell plot.

2. Buckling Load and Buckling Behaviors

When a rectangular thin plate shown in Fig. 1 is subjected to sufficiently small magnitude of in-plane compressive loads, the plate is in equilibrium. The panel remains flat, and compressive strain is observed on both sides of the specimen. As the

magnitude of the in-plane loads increase, the plate configuration is changed to non-flat configuration and become unstable. In-plane strains on the convex side of the specimen change to tensile strain. The magnitude of compressive load at which the plate becomes unstable is called the "critical buckling load." The buckling load is governed by a differential equation written as [1]

$$\frac{\partial^4 w}{\partial x^4} + 2 \frac{\partial^4 w}{\partial x^2 \partial y^2} + \frac{\partial^4 w}{\partial y^4} = \frac{1}{D} N_x \frac{\partial^2 w}{\partial x^2} \quad (1)$$

where $D = \frac{Eh^3}{12(1-\nu^2)}$

For a simply-supported plate, critical buckling load can be determined, analytically, as:

$$N_{cr} = \frac{\pi^2 D}{a^2 m^2} \left[m^4 + 2(mnR)^2 + (nR)^4 \right] \quad (2)$$

where $R = a/b$ (aspect ratio)
 m and n are positive integer number representing the buckling mode

The buckling load is determined from the minimum value of N_{cr} determined from eq.(2).

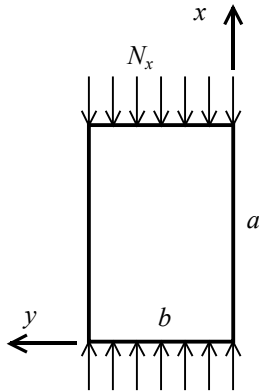


Fig. 1 A rectangular plate subjected to a uniaxial in-plane load

Theoretically, the buckling phenomenon may be described from a plot of the out-of-plane displacement (w) at a specific point, i.e. point of maximum displacement, against in-plane load (N_x), as shown in Fig 2. In classical linear buckling theory, when in-plane load increases from zero, an out-of-plane displacement remains zero, and a load-displacement curve follows Path 1 until buckling load is reached. At this point, which is called a bifurcation point, the load-displacement curve may follow Path 2 which is a theoretical linear buckling path. Buckling load (N_{cr}) can

be obtained from classical linear buckling theory as shown in Eq.(2). The critical buckling load is defined on this horizontal line. In a nonlinear theory, the curve follows Path 3, which is called a "postbuckling" curve. This curve is important in the study of plate behavior beyond the buckling load. However, for a real plate with initial imperfections, the curve will not follow Path 1, i.e. an out-of-plane displacement occurs as soon as load N_x is applied. In this case, the load-displacement curve follows Path 4 from the beginning of the loading.

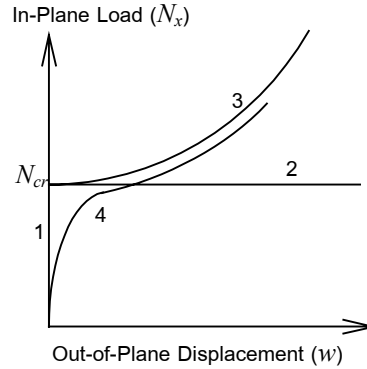


Fig 2 Buckling phenomenon represented by a plot of N_x vs. w

Besides theoretical studies, buckling phenomenon has been in the interest of many researchers. Several concepts of test setup have been proposed and studied [5]. One of the important issues considered in the experiment involves in the method of identifying a buckling load of the test specimen. Since plates used in the experiment and their boundary conditions are not perfect, a bifurcation point cannot be evidently observed during the experiment. There are several techniques of identifying the buckling load in the experiment used in the past studies. Four of the methods which are examined in the present study are graphically shown in Fig. 3-6. For the first two methods, i.e. plot of applied load vs. out-of-plane displacement and plot of end shortening vs. out-of-plane displacement, buckling load is determined from the intersection of two tangents drawn on the curve in the pre-buckling and post-buckling regions. The third method in Fig.5 or average strain method utilizes the fact that in-plane strain on one side of the specimen becomes tensile strain when the specimen is buckled. In this method, the applied load is plotted against the algebraic mean compressive strain, $\epsilon_A = (\epsilon_1 + \epsilon_2)/2$, where ϵ_1 and ϵ_2 are in-plane strains on both sides of the specimen. The buckling load is determined from a sufficiently shape break of the plot. This method is documented as a simple and effective technique which does not required any data in the post-buckling region. The Southwell plot is a plot between a ratio

of out-of-plane displacement and applied load (w/N_x) vs. the out-of-plane displacement. Buckling load is determined from 1/slope of the plot. In the present study, buckling loads of aluminum rectangular plates determined from four methods outlined above are compared to each other and to the theoretical solutions.

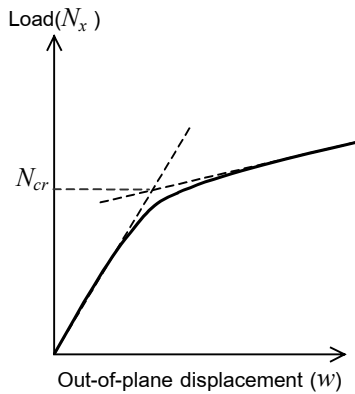


Fig. 3 Buckling load from a plot of N_x vs. w

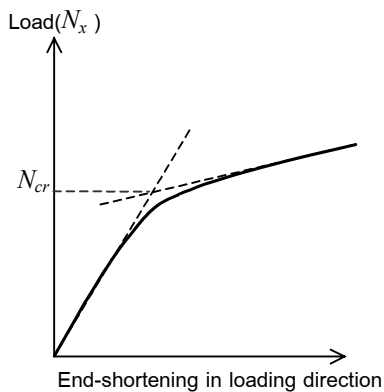


Fig. 4 Buckling load from a plot of N_x vs. end-shortening

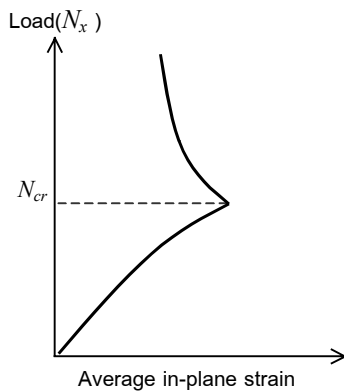


Fig. 5 Buckling load from a plot of N_x vs. average strain

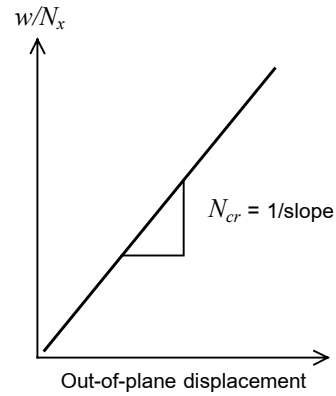


Fig. 6 Buckling load from a plot of w/N_x vs. w (Southwell plot)

3. Experiment Setup

In this study, three aluminum rectangular plates were tested for buckling loads using four techniques as stated previously. The test panels were mounted on a specially designed loading frame and subjected to compressive loading as shown in Fig 7. Compressive loads were vertically applied by a hydraulic cylinder onto the movable crosshead. The movable crosshead can be moved vertically on four circular columns with supports from linear bearings embedded in the crosshead. Applied compressive load was monitored by a 10-ton load cell placed on top of the crosshead. The simple support boundary conditions were enforced on four edges of the specimen as shown in Fig. 8. The top and bottom sides of the specimen were placed into a slot of a circular slotted rod, which was placed into a semi-circular slot of the crossheads, Fig. 8(a). With this configuration, the test panels are allowed to rotate, but restrained to move in the out-of-plane direction. For the side supports, two knife-edge supports were placed on the specimen to simulate the simple support as shown in Fig. 8(b). Similar to the top and bottom supports, side edges of the specimen can rotate, but cannot move out of plane. The out-of-plane displacements and end shortening were measured using dial indicators, while strain gages were mounted on both sides of the specimens at the position of maximum out-of-plane displacement to monitor the in-plane strains.

A total of three rectangular aluminum plates, namely A, B, and C, were tested in this study. The width (b) of all panels is 24 cm with heights (a) of 24, 36, and 48 cm, respectively. The specimens were tested under uniaxial compressive loading. Applied compressive loads, maximum out-of-plane displacements, end shortenings, and in-plane strains were measured and plotted according to the technique mentioned previously. Strain gages used to measure in-plane strains were attached at the point of theoretical maximum out-of-plane displacement, i.e. at the middle of the plate for specimen A and at one-fourth of the height for

specimen B and C. These locations are determined from the theoretical buckling modes which are mode 1 for specimen A and mode 2 for specimen B and C. Dial indicator was also placed adjacent to the strain gage. Aluminum used in this experiment is tested for Young's modulus and Poisson's ratio, and they are 65 GPa and 0.3, respectively. These properties are used to determine the theoretical buckling load according to Eq.(2).

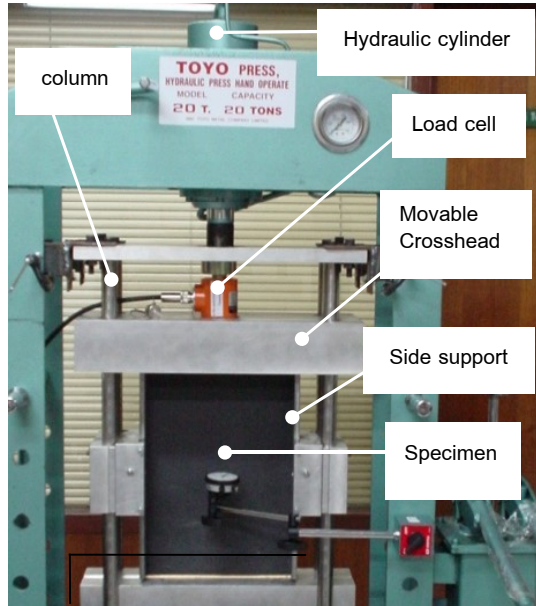


Fig. 7 The compression test frame for buckling experiment

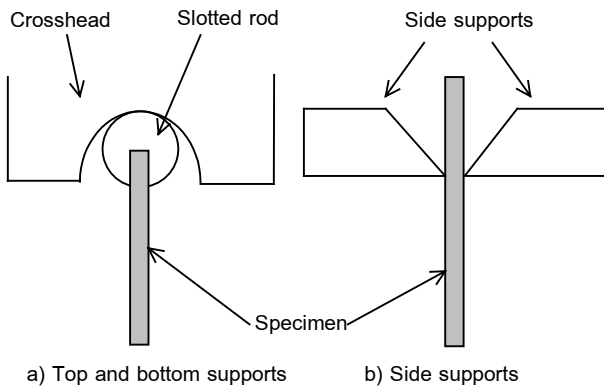


Fig. 8 The schematic of simply supported boundary condition

4. Experimental result

Experimental buckling loads were identified from the plots. They are compared to the theoretical solution and to each other in Table 1. Although, the resolution of the load cell used in this experiment is 0.01 kN, the experimental buckling loads is reported with a resolution of 1 kN because the data reduction processes depend on human's judgment more than mathematical technique. The plot of end shortening for the smallest specimen

is almost straight, so the buckling load from this method is not applicable. The example plots of the four techniques for specimen C are shown in Fig. 9-12.

Table 1. Experimental and theoretical buckling load

Specimen (a x b)	Theory (kN/m)	Experiment (kN/m)			
		I	II	III	IV
A (24x24)	39.98	25	N/A	40	55
B (36x24)	43.38	42	44	43	50
C (48x24)	39.98	36	41	40	65

Note: I = plot of applied load vs. out-of-plane displacement
 II = plot of applied load vs. end shortening
 III = plot of applied load vs. average strain
 IV = the Southwell plot

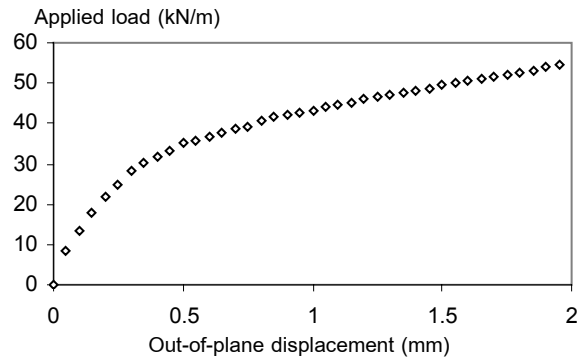


Fig. 9 Plot of applied load vs. out-of-plane displacement for specimen C

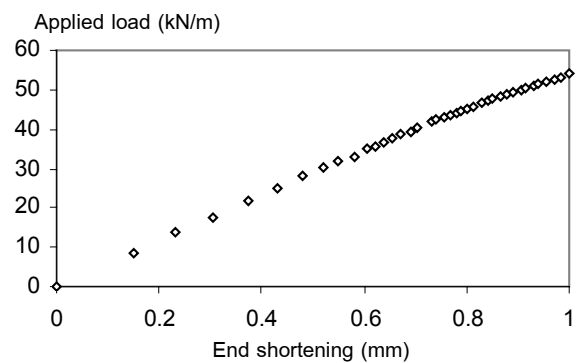


Fig. 10 Plot of applied load vs. end shortening for specimen C

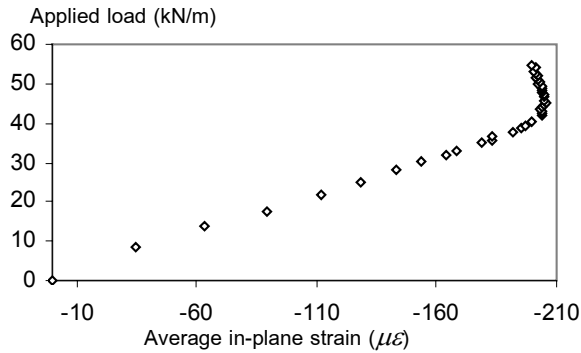


Fig. 11 Plot of applied load vs. average strain for specimen C

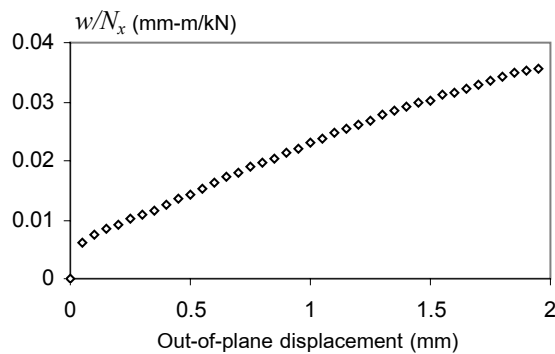


Fig. 12 The Southwell plot for specimen C

5. Discussion and conclusion

From the experiment result shown in Table 1, experimental buckling load of specimen A is not well measured by method I and method II. The plot of maximum displacement shows unusually low buckling load compared to the theoretical one. The plot of end shortening does not have a clear change of slope, and buckling load could not be obtained from this technique. No explanation or conclusion can be made about these two measurements on specimen A because there is not enough experiment data. More experiments on specimens with the same size should be conducted before any firm conclusions can be made.

Experimental buckling loads from first three methods have the same trend as those of the theoretical ones. That is buckling loads of specimen A and C are identical and lower than that of specimen B. Although technique I and II do not return a good buckling load for the smallest specimen, the buckling loads of specimen B and C determined from these techniques have a good trend compared to the theoretical solutions. For the Southwell plot, buckling loads for all specimens are much higher than the theoretical predictions. Moreover, buckling loads of all specimens do not have the same tendency as those of the theoretical solutions. Buckling load of specimen B should be

higher than those of the other two, but the experiments showed otherwise. Therefore, Southwell plot does not give an acceptable result from the experiments on these three specimens.

The plots of applied load vs. average strain provide a very good experiment results compared with the theoretical solutions. The difference between experimental and theoretical buckling loads is less than 1%. However, it is too early to conclude that the plot of applied load vs. average strain is the best technique to identify buckling point. More experiments should be conducted before a more concrete conclusion can be made.

Plots of applied load vs. out-of-plane displacement, Fig. 9, show a clear change of the slope in the pre-buckling and post-buckling region, as expected. Two lines tangent to experimental data can be drawn, comfortably, although out-of-plane deflection can be observed as soon as a compressive load is applied. This observation suggests that there are imperfections in the experimental setup. On the other hand, the configuration of the plots of applied load vs. end shortening is different from those suggested in the literature [5]. The change of slope is not easily seen compared to that of the plot of out-of-plane displacement. This probably is an effect of imperfection, as well. For average strain method, an abrupt change of the curve, as expected, is obtained. It is easy to identify the buckling load compared to the first two methods. For the Southwell plot, the experiment data forms a straight line, but does not intersect the origin, and the buckling load is higher than the theoretical solution in all cases.

In conclusion, a compressive test frame is designed and built to accommodate the buckling experiments. Three rectangular aluminum plates were tested for critical buckling loads using four techniques usually used in the literatures. With the available experiment data, a plot of average strain method is the most reliable technique, while a plot of out-of-plane displacement and a plot of end shortening show a good tendency of determined buckling loads. The experiment also showed that the Southwell plot is less dependable. More experiments will be performed so that a solid conclusion about advantages and disadvantages of each technique can be made with confidence.

6. Acknowledgement

This research is supported by the Thailand Research Fund under project grant No. MRG4580003.

References

- [1] Brush, D. O. and Almroth, B. O., "Buckling of bars, plates, and shells," McGraw-Hill, New York, 1975.

- [2] Chai, G.B., Banks, W.M., and Rhodes, J., "The instability behaviour of laminated panels with elastically rotationally restrained edges," *Composite Structures*, 19, pp.41-65 (1991).
- [3] Chai, G.B., Hoon, K.H., and Chin, S.S., "Buckling response of symmetric laminated plates," *Mechanics of Structures and Machines*, 24, pp.439-52 (1996).
- [4] Tuttle, M., Singhatanadgid P., and Hinds, G., "Buckling of Composite Panels Subjected to Biaxial Loading," *Experimental Mechanics*, 39, pp.191-201 (1999).
- [5] Singer, J., Arbocz, J., and Weller, T., "Buckling Experiments: Experimental methods in buckling of thin-walled structures," John Wiley & Sons Inc., New York, 2002.